



# Bisphenol A modulates proliferation, apoptosis, and wound healing process of normal prostate cells: Involvement of G2/M-phase cell cycle arrest, MAPK signaling, and transcription factor-mediated MMP regulation

Jun-Hui Song<sup>a</sup>, Byungdo Hwang<sup>a</sup>, Su-Bin Kim<sup>a</sup>, Yung Hyun Choi<sup>b</sup>, Wun-Jae Kim<sup>c</sup>, Sung-Kwon Moon<sup>a,\*</sup>

<sup>a</sup> Department of Food and Nutrition, Chung-Ang University, Anseong 17546, Republic of Korea

<sup>b</sup> Department of Biochemistry, College of Oriental Medicine, Donggeui University, Busan 47340, Republic of Korea

<sup>c</sup> Department of Urology, Chungbuk National University, Cheongju, Chungbuk 361-763, Republic of Korea

## ARTICLE INFO

Edited by Dr. Caterina Faggio

### Keywords:

Bisphenol A  
Prostate cells  
Cell cycle  
Wound healing process  
MMP-9

## ABSTRACT

Bisphenol A (BPA) is commonly used to produce epoxy resins and polycarbonate plastics. BPA is an endocrine-disrupting chemical that is leaked from the polymer and absorbed into the body to disrupt the endocrine system. Although BPA may cause cytotoxicity in the prostate, a hormone-dependent reproductive organ, its underlying mechanism has not yet been elucidated. Here, we investigated the effects of BPA on cell proliferation, apoptosis, and the wound healing process using prostate epithelial cells (RWPE-1) and stromal cells (WPMY-1). Observations revealed that BPA induced G2/M cell cycle arrest in both cell types through the ATM–CHK1/CHK2–CDC25c–CDC2 signaling pathway, and the IC<sub>50</sub> values were estimated to be 150 μM. Furthermore, BPA was found to induce caspase-dependent apoptosis through initiator (caspase-8 and –9) and executioner (caspase-3 and –7) caspase cascades. In addition, BPA interfered with the wound healing process through inhibition of MMP-2 and –9 expression, accompanied by reductions in the binding activities of AP-1 as well as NF-κB motifs. Phosphorylation of MAPKs was associated with the BPA-mediated toxicity of prostate cells. These results suggest that BPA exhibits prostate toxicity by inhibiting cell proliferation, inducing apoptosis, and interfering with the wound healing process. Our study provided new insights into the precise molecular mechanisms of BPA-induced toxicity in human prostate cells.

## 1. Introduction

Bisphenol A (BPA) is an organic synthetic compound commonly used to produce plastic polymers, such as polycarbonates, epoxy resins, and polyvinyl chloride (Erickson, 2008; Fiege et al., 2000). These polymers are commercially used for baby bottles, food containers, water bottles, the linings of food and beverage cans, dental sealants, and many other daily necessities products (Brede et al., 2003; Welshons et al., 2006). Polymer-derived chemicals, such as BPA, can be released into the environment and absorbed into the body through diet and oral or dermal contact. Due to its wide use in industrial products, BPA is a widespread environmental pollutant. Some studies have recorded more than 1 mg/kg of BPA in vegetables, which is suggested to be caused by BPA migration from plastic irrigation devices (Wilson et al., 2007; Zalko et al., 2011). The U.S. Centers for Disease Control and Prevention have

estimated that 92.6% of Americans have measurable levels of BPA in urine, indicating the high potential for continuous BPA exposure (Calafat et al., 2005).

BPA is a representative endocrine-disrupting chemical that alters the function of the endocrine system by mimicking the action of estrogen (Erickson, 2008). BPA binds to estrogen receptor (ER) subtypes (ER $\alpha$ , ER $\beta$ , and ER $\gamma$ ) and interferes with estrogenic signaling pathways, and it also targets the androgen receptor (AR) function, disrupting AR-mediated signaling (Rehan et al., 2015; Teng et al., 2013). Thus, the adverse effects of BPA are extensive, and exposure to BPA generally correlates with an elevated risk of reproductive system diseases, such as prostate and prostatic diseases (Davis-Dao et al., 2007; Huang et al., 2018; Kidani et al., 2017).

The prostate is a hormone-dependent reproductive organ, and both androgens and estrogens play key roles in prostate function,

\* Correspondence to: Department of Food and Nutrition, Chung-Ang University, 4726 Seodong-Daero, Daedeok-Myeon, Anseong 17546, Republic of Korea.  
E-mail address: [sumoon66@cau.ac.kr](mailto:sumoon66@cau.ac.kr) (S.-K. Moon).

homeostasis, and diseases (Huang et al., 2018; Roehrborn, 2008; Siegel et al., 2020). BPA has been qualified as a xenoestrogen and thus has the potential to adversely affect the prostate (Bilancio et al., 2017; Huang et al., 2018; Takahashi and Oishi, 2003; Wu et al., 2011). A previous study showed that prostate weight decreased in male rats administrated BPA at 235 mg/kg/day, and even less than 20 mg/kg/day of BPA induced toxicity of the prostate gland (Takahashi and Oishi, 2003). In addition, BPA can induce cell cycle arrest in prostate cancer cells through activation of the MAPK/p53 signaling pathway (Bilancio et al., 2017). BPA can also induce oxidative stress and DNA damage, producing cytotoxic effects on prostate epithelial cells (RWPE-1) (Kose et al., 2020). Although accumulating evidence indicates that BPA has the potential to cause cytotoxicity in the prostate, the exact mechanism remains largely unresolved.

To treat benign prostatic hyperplasia or prostate cancer, thulium laser therapy or tissue resection has been performed (Barbalat et al., 2016; Sun et al., 2020; Wang et al., 2017). However, these therapies are inevitably a crucial source of necrotic tissue and secondary sloughing, which causes complications (Sun et al., 2020; Wang et al., 2017). Prompt wound healing after surgery is important because such complications persist until the prostate urethral wound is completely healed (Sun et al., 2020; Wang et al., 2017). Dietary exposure to BPA has been shown to delay wound healing by suppressing ovarian estrogen secretion (Wen et al., 2022). Therefore, it is considered that BPA could interfere with the wound healing process in the prostate, although the underlying mechanism has not yet been identified.

We aim to elucidate the mechanism by which BPA exerts adverse effects on cell proliferation and the wound healing process. To this end, we evaluated the effects of BPA on the viability of RWPE-1 and stroma cells (WPMY-1). In addition, we examined the potential action mechanism of BPA toxicity associated with G2/M cell cycle arrest, caspase-mediated apoptosis, multiple signaling pathways, and metastatic potential.

## 2. Materials and methods

### 2.1. Materials

Polyclonal antibodies specific to p-ATR, ATR, p-ATM, ATM, p-CHK1, CHK, p-CHK2, CHK2, p-CDC25C (S216), CDC25C, p-CDC2 (T14/Y15), CDC2, caspase-3, caspase-7, caspase-8, caspase-9, p-AKT, AKT, p-ERK, ERK, p-JNK, JNK, p-p38, and p38 were purchased from Cell Signaling (Danvers, MA, USA). Polyclonal antibodies specific to cyclin A, cyclin B, DR4, DR5, FAS, TRAIL, BAX, Bcl-2, XIAP, PARP-1, Z-VAD-FMK, and actin were purchased from Santa Cruz Biotechnology (Santa Cruz, CA, USA). Polyclonal antibodies specific to MMP-2 and MMP-9 were purchased from Sigma-Aldrich (St Louis, MO, USA).

### 2.2. Cell culture

The human normal prostate cell lines WPMY-1 and RWPE-1 were purchased from the American Type Culture Collection (ATCC, Manassas, VA, USA). All materials for cell culture were purchased from Gibco (Carlsbad, CA, USA). WPMY-1 cells were cultured in RPMI 1640 culture media containing 10% fetal bovine serum (FBS), 100 U/mL penicillin, and 100 µg/mL streptomycin. RWPE-1 cells were cultured in keratinocyte serum-free medium (K-SFM) containing keratinocytes supplements, in addition to 100 U/mL penicillin and 100 µg/mL streptomycin. Both cell lines were incubated at 37 °C in a humidified incubator with 5% CO<sub>2</sub>.

### 2.3. Cell viability

Cell counting and 3-(4,5-dimethylthiazol-2-yl)-2,5-diphenyltetrazolium bromide (MTT) assays were performed to measure cell viability, as described previously (Park et al., 2015). All materials for

both assays were purchased from Sigma-Aldrich. WPMY-1 and RWPE-1 cells ( $5 \times 10^3$ /well) were plated in 96-well plates and incubated at 37 °C for 18 h. The cells were treated with 0, 100, 150, and 200 µM BPA for 24 h. After incubation, 10 µL MTT (5 mg/mL solution) was added to each well and reacted for 4 h. After replacing the medium with dimethyl sulfoxide (DMSO), the absorbance at 540 nm was measured using a fluorescence microplate reader. For the cell counting assay, 100 µL of detached cells was combined with 80 µL of 0.4% trypan blue. After gentle pipetting, cells were counted using a hemocytometer. Cells were measured by the equation: % viable cells =  $[1 - (\text{number of blue cells} / \text{number of total cells})] \times 100$ .

### 2.4. Cell cycle and apoptosis analyses

Cell cycle and apoptosis analyses were determined using the Muse™ Cell Analyzer (Merck Millipore, Billerica, MA, USA) according to the manufacturer's instructions. Briefly, for cell cycle analysis, harvested cells were fixed in 70% ethanol at -20 °C. Afterward, the cells were washed twice with PBS, and then 200 µL of propidium iodide (PI) containing Muse™ Cell Cycle Reagent (MCH100106, Merck Millipore) was added. After incubation at room temperature for 30 min in the dark, the percentage of cells in each cell cycle phase was measured by detecting PI levels. For apoptosis analysis, the Muse™ Annexin V and Dead Cell Reagent (MCH100105, Merck Millipore) was used to stain the harvested cells. After incubation at room temperature for 20 min, the cell apoptotic rate was analyzed.

### 2.5. Terminal deoxynucleotidyl transferase dUTP nick end labelling (TUNEL) assay

Both cells were cultured with various concentrations of BPA for 24 h. Cells were washed with PBS and fixed in a fixation solution (4% paraformaldehyde in 1 × PBS at pH 7.4) for 1 h. Then, the cells were incubated with permeabilizing solution (0.1% Triton X-100 in 0.1% sodium citrate) for 5 min. Subsequently, cells were stained with TUNEL detection solution (Roche, Indianapolis, IN) for 1 h at 37 °C in the dark. The stained cells were observed under a fluorescence microscope.

### 2.6. Immunoblot assay

The immunoblot assay was accomplished as described previously (Park et al., 2015). Briefly, the protein was extracted from the cells using RIPA lysis buffer. The concentration of protein was determined by the BCA Protein Assay Reagent Kit (Thermo Fisher Scientific, Waltham, MA, USA). The protein (20–30 µg each) was loaded on a sodium dodecyl sulfate (SDS, 0.1%)–polyacrylamide gel and resolved by SDS-polyacrylamide gel electrophoresis (SDS-PAGE). The electrophoresed protein was transferred to nitrocellulose membranes (Hybond, GE Healthcare Bio-Sciences, Marlborough, MA, USA). After blocking with 5% skim milk, the membranes were incubated with primary antibodies for 18 h and secondary antibodies for 2 h. The immunocomplexes were detected by the electrochemiluminescence (ECL) reagent (Super-Signal® West Pico Chemiluminescent Substrate, Thermo Fisher Scientific).

### 2.7. Wound healing migration assay

The wound healing migration assay described by Park et al. (2015) was performed. Briefly, WPMY-1 and RWPE-1 cells ( $4 \times 10^5$  cells/well) were plated in 6-well plates. When cells were 90% confluent, the cell surface area was scraped with a 200 µL pipette tip to create a wound. After washing twice with culture media, the plate was incubated with culture media containing 0, 25, 50, and 100 µM BPA for 24 h. The wound closure was monitored with an inverted microscope at 40 × magnification.

2.8. Boyden chamber invasion assay

The Boyden chamber invasion assay detailed by Park et al. (2015) was performed. Briefly, Transwell® chambers coated with BD Matrigel Basement Membrane Matrix (BD Biosciences, San Diego, CA, USA) were used. WPMY-1 and RWPE-1 cells ( $5 \times 10^4$  cells/well) were seeded with 0, 25, 50, and 100  $\mu\text{M}$  BPA in the upper chamber. The medium containing 10% FBS was filled in the lower chamber. After 24 h, the cells in the membrane of the upper chamber were fixed with 4% paraformaldehyde and then stained with 0.01% crystal violet. The density of invading cells was photographed and analyzed using ImageJ.

2.9. Zymography

Zymography was performed as reported previously (Park et al., 2015). The conditioned medium was mixed with the non-reducing SDS sample buffer and then electrophoresed on an 8% polyacrylamide gel containing 0.2% gelatin. The gel was soaked twice in 2.5% Triton X-100 at room temperature for 15 min and incubated in an incubation buffer (50 mM Tris-HCl [pH 7.5], 150 mM NaCl, and 10 mM  $\text{CaCl}_2$ ) at 37 °C for 24 h. The gel was washed twice with distilled water, stained with 0.2% Coomassie blue staining buffer for 30 min, and destained with 10% acetic acid destaining buffer until the white bands were visualized. The white bands were photographed and analyzed using ImageJ.

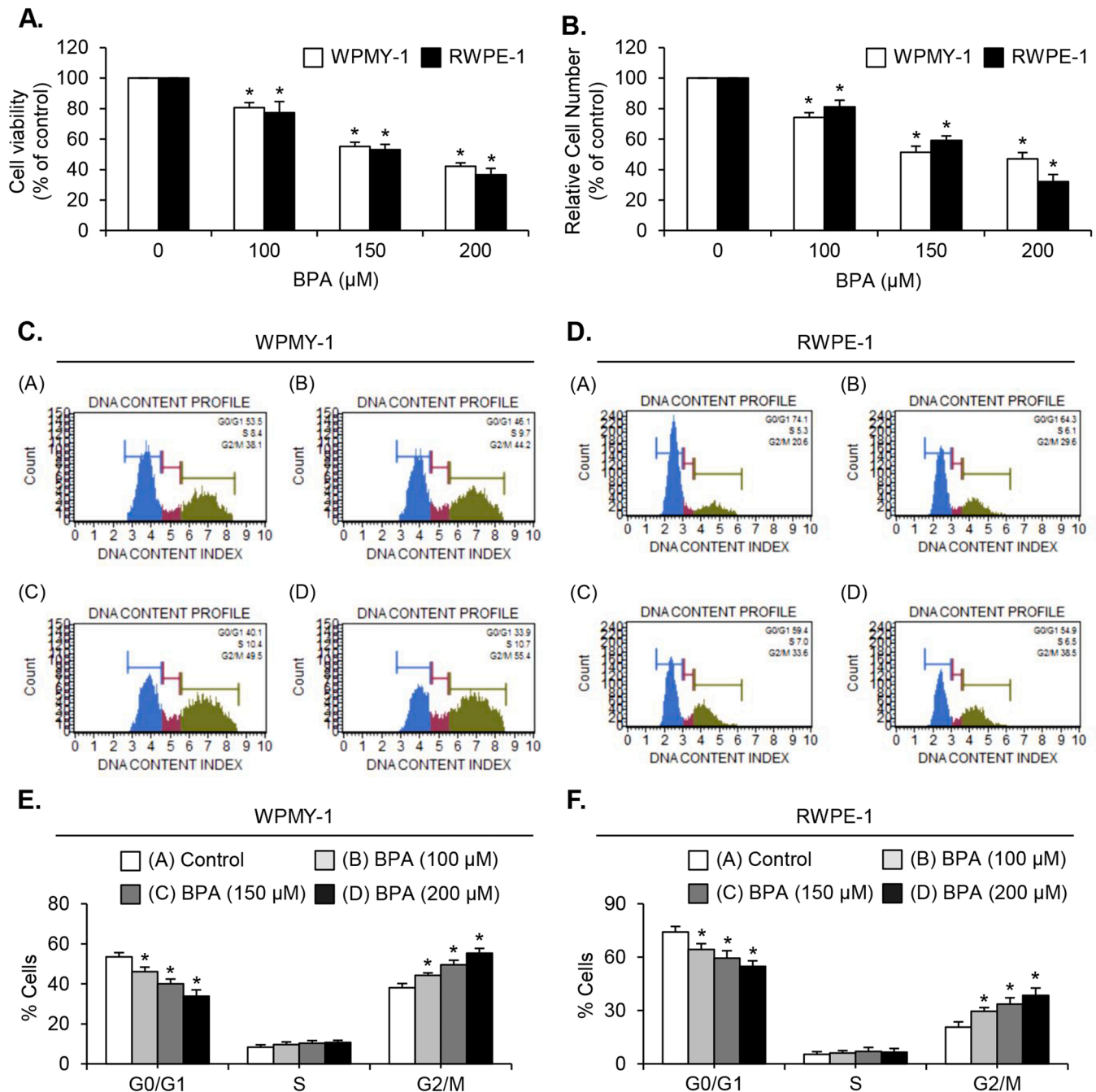


Fig. 1. BPA inhibits the proliferation of normal prostate cells through G2/M cell cycle arrest. WPMY-1 and RWPE-1 cells were treated with 0, 100, 150, and 200  $\mu\text{M}$  BPA for 24 h. MTT assay (A) and cell counting (B) were conducted to measure cell viability. (C, D) Cell cycle distribution of both cell types treated with BPA for 24 h was analyzed by flow cytometry. (E, F) Histograms present the percentage of cells in G0/G1, S, and G2/M phases. Results are shown as mean  $\pm$  SEM (n = 3 independent experiments). Asterisks indicate significant differences (Student's *t*-test,  $P < 0.05$ ).

## 2.10. Electrophoretic mobility shift assay (EMSA)

EMSA experiments were performed, essentially as reported previously (Park et al., 2015). The cells were suspended in lysis A buffer (10 mM HEPES [pH 7.9], 10 mM KCl, 0.1 mM EDTA, 0.1 mM EGTA, 0.5% NP-40, 1 mM DTT, and 0.5 mM PMSF) for 15 min at 4 °C. The nuclear pellet was collected by centrifugation (13,000 × g), followed by extraction in lysis B buffer (20 mM HEPES [pH 7.9], 400 mM NaCl, 1 mM DTT, 1 mM PMSF, 1 mM EDTA, and 1 mM EGTA) at 4 °C for 15 min. The concentration of the nuclear extract was determined by the BCA Protein Assay Reagent Kit (Thermo Fisher Scientific). The nuclear extract (5–10 µg) was mixed with binding reaction solution (25 mM HEPES buffer [pH 7.9], 0.5 mM EDTA, 0.5 mM DTT, 0.05 M NaCl, 2.5% glycerol, 2 µg poly(dI-dC), and 5 fmol (2 × 10<sup>4</sup> cpm) of a Klenow end-labeled (32 P-ATP) 30-mer oligonucleotide, which spanned the DNA binding site of the MMP-2 and -9 promoter) for 20 min at room temperature. The reaction mixture was electrophoresed on a 6% polyacrylamide gel at 4 °C. The gel was dried and exposed to X-ray film for 24–48 h. The bands were analyzed using ImageJ.

## 2.11. Statistical analysis

All experiments were independently performed at least three times. The Student's *t*-test was used to analyze the statistical significance ( $P < 0.05$ ) among groups.

## 3. Results

### 3.1. BPA inhibits the proliferation of normal prostate cells via induction of G<sub>2</sub>/M cell cycle arrest

To demonstrate the antiproliferative activity of BPA in normal prostate cells, WPMY-1 and RWPE-1 cells were treated with BPA (0, 100, 150, and 200 µM) for 24 h, and then MTT and cell counting assays were performed. As shown in Fig. 1A and B, the proliferative ability of both cell types decreased in a dose-dependent manner. The IC<sub>50</sub> values of BPA in both cell types were estimated to be 150 µM. Furthermore, we

ascertained whether BPA could induce cell cycle arrest. Both cell types were treated with various concentrations of BPA (0, 100, 150, and 200 µM) for 24 h, and the DNA contents were determined by flow cytometry analysis. BPA treatment increased the population of G<sub>2</sub>/M phase cells from 38.1% to 55.4% in WPMY cells (Fig. 1C and E). In case of G<sub>0</sub>/G<sub>1</sub>-phase, cell numbers reduced from 53.5% to 33.9%. In RWPE cells, BPA diminished the proportion of G<sub>0</sub>/G<sub>1</sub>-phase cells (from 74.1% to 54.9%) and augmented the population of G<sub>2</sub>/M-phase cells (from 20.6% to 38.5%) (Fig. 1D and F). However, BPA did not affect S-phase population in both cells (Fig. 1C-F). In both cell types, BPA treatment significantly accumulated cells in the G<sub>2</sub>/M phase, indicating cell cycle arrest (Fig. 1C - F). These results suggest that the antiproliferative activity of BPA may be associated with G<sub>2</sub>/M cell cycle arrest in normal prostate cells.

### 3.2. BPA induces G<sub>2</sub>/M cell cycle arrest via ATM-mediated CHK1/CHK2–CDC25c–CDC2 pathway in normal prostate cells

To elucidate the mechanism for G<sub>2</sub>/M cell cycle arrest in BPA-treated normal prostate cells, we tested the expression and phosphorylation of G<sub>2</sub>/M cell cycle regulatory proteins by immunoblotting. In both WPMY-1 and RWPE-1 cells, BPA strongly induced the phosphorylation of CHK1 and CHK2 through activation of ATM despite a reduction in the total ATM, CHK1, and CHK2 proteins (Fig. 2A and C, Fig. S1A and C). However, activation of ATR was not observed in both cell types (Fig. 2A and C, Fig. S1A and C). In addition, the inhibitory phosphorylation of CDC25c (Ser-216) was increased in both cell types treated with BPA (Fig. 2B and D, Fig. S1B and D). BPA treatment induced phosphorylation of CDC2 on the Thr-14/Tyr-15 residue in both cell lines (Fig. 2B and D, Fig. S1B and D). Treatment with BPA reduced the expression of cyclin A, cyclin B, CDC25c, and CDC2 (Fig. 2B and D, Fig. S1B and D). Our data confirmed that BPA induces G<sub>2</sub>/M cell cycle arrest via the ATM–CHK1/CHK2–CDC25c–CDC2 signaling pathway in normal prostate cells.

### 3.3. BPA induces caspase-dependent apoptosis in normal prostate cells

To elucidate whether BPA causes apoptosis in normal prostate cells, we performed flow cytometry analysis to measure the apoptosis rate.

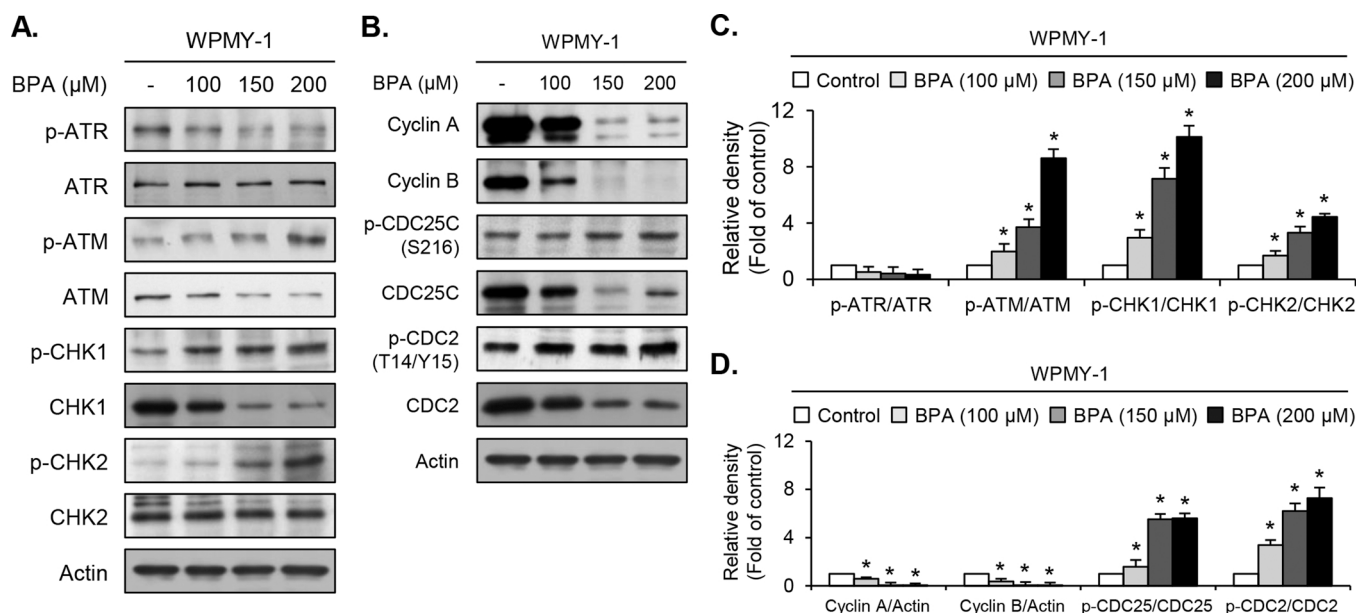


**Fig. 2.** Expression of differentially regulated G<sub>2</sub>/M-phase cell cycle-associated proteins in prostate cells by BPA. WPMY-1 cells were treated with 0, 100, 150, and 200 µM BPA for 24 h. (A, C) Immunoblot analysis for antibodies specific for p-ATR, ATR, p-ATM, ATM, p-CHK1, CHK1, p-CHK2, CHK2, and actin. (B, D) Expression levels of Cyclin A, cyclin B, p-CDC25C, CDC25C, p-CDC2, CDC2, and actin were analyzed via immunoblot analysis. All graphs represent the fold change in phosphorylation rates or expression level compared to controls, shown as mean ± SEM (n = 3 independent experiments). Asterisks indicate significant differences (Student's *t*-test,  $P < 0.05$ ).

Following treatment with BPA (0, 150, 200, and 250  $\mu\text{M}$ ) for 24 h, WPMY-1 and RWPE-1 cells were stained with annexin V and propidium iodide (PI). Our data indicated that BPA significantly induces apoptosis in a dose-dependent manner, and the apoptosis rate (as the sum of early apoptosis and late apoptosis) was increased in both cell lines to 57.8% and 12.85%, respectively, after treatment with 250  $\mu\text{M}$  BPA (Fig. S2A-D). Next, TUNEL assay was conducted to confirm the apoptosis induction of BPA in both cells. TUNEL assay revealed apoptotic features with increasing BPA concentration (Fig. S2E and F). To understand the mechanism underlying BPA-induced apoptosis, regulation of apoptosis-related proteins was verified by immunoblotting. In both cell lines, BPA significantly increased the expression of DR4, DR5, and FAS, which are apoptosis-related receptors (Fig. 3A and C, Fig. S3A and C). The expression of TRAIL, a ligand of DR4 and DR5, was also increased (Fig. 3A and C, Fig. S3A and C). Additionally, the BAX expression was increased in both BPA-treated normal prostate cell lines, whereas the expression of Bcl-2 was decreased in a dose-dependent manner (Fig. 3A and C, Fig. S3A and C). The level of XIAP expression decreased in both BPA-treated cell lines (Fig. 3A and C, Fig. S3A and C). Treatment with BPA induced PARP1 cleavage by decreasing the levels of full-length

PARP1 (Fig. 3A and C, Fig. S3A and C). Moreover, we observed activation of initiator caspase-8 and -9 after treatment with 200 and 250  $\mu\text{M}$  BPA (Fig. 3B and D, Fig. S3B and D). Furthermore, both BPA-treated cell lines demonstrated a decrease in full-length caspase-3 and -7, accompanied by increases in their cleaved forms (Fig. 3B and D, Fig. S3B and D). Finally, Z-VAD-FMK (a caspase-3 inhibitor) was used to investigate direct apoptosis induction of BPA in prostate cells, since BPA stimulated activation of caspase-3 in both cells (Fig. 3B and Fig. S3B). BPA-induced apoptosis was markedly suppressed in the presence of Z-VAD-FMK (Fig. 3E and F and Fig. S3E and F). These results illustrate that treatment with BPA induces caspase-dependent apoptosis in normal prostate cells.

### 3.4. BPA induces phosphorylation of MAPKs in normal prostate cells

To investigate whether the BPA-mediated antiproliferative effect is involved in the MAPK (ERK, p38, and JNK) and AKT signaling pathways, WPMY-1 and RWPE-1 cells were treated with BPA (0, 100, 150, and 200  $\mu\text{M}$ ) for 30 min and then the phosphorylation level was measured by immunoblotting. While BPA treatment increased the

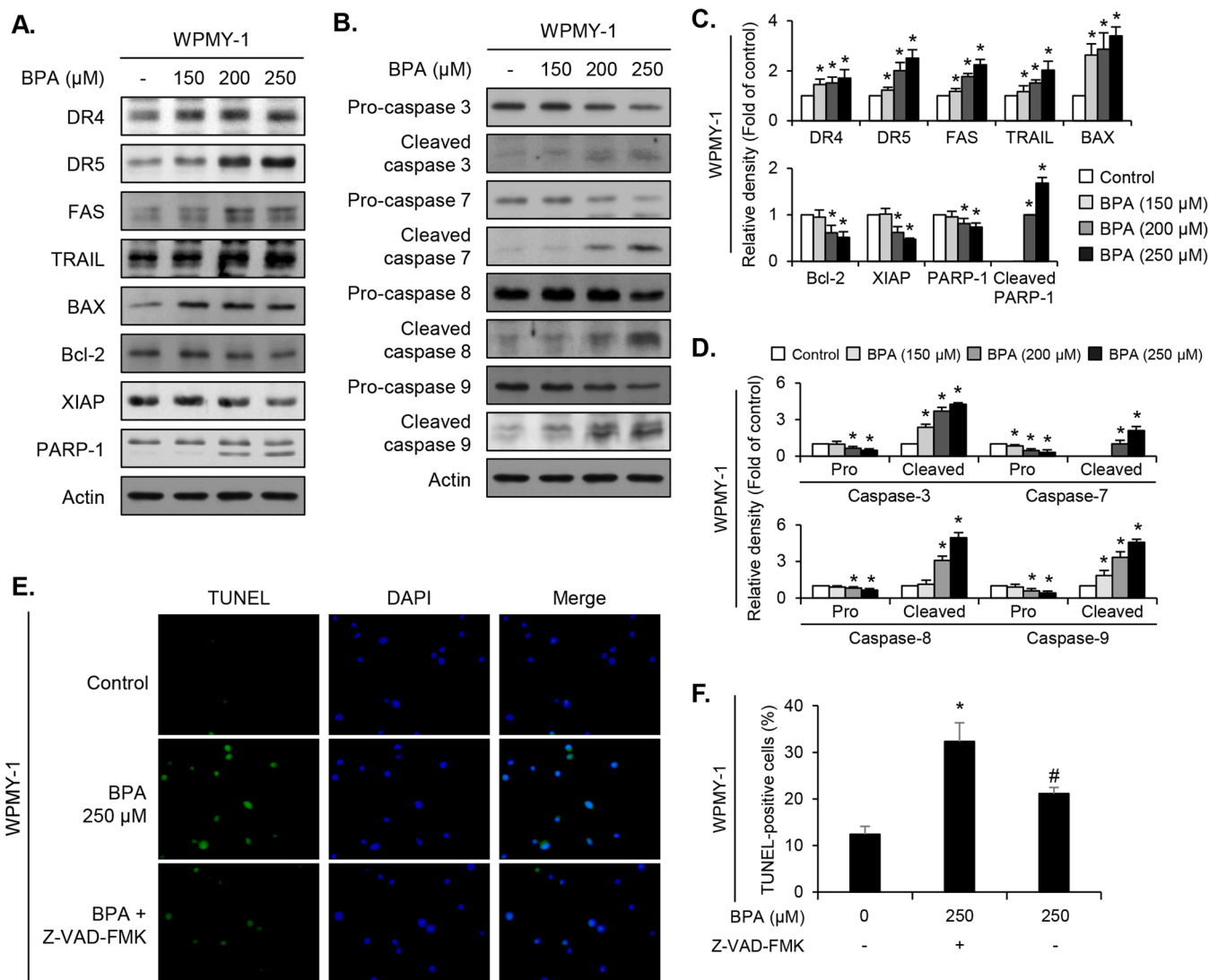


**Fig. 3.** Effect of BPA on apoptosis signaling in normal prostate cells. WPMY-1 cells were treated with 0, 150, 200, and 250  $\mu\text{M}$  BPA for 24 h. (A, C) Representative immunoblot analysis shows the expression level of apoptosis-regulatory proteins altered by BPA. (B, D) Caspase cleavage was measured by immunoblot analysis. All bar graphs show the quantitative analyses of the intensities of the bands. Expression levels were normalized by corresponding actin intensity. (E, F) WPMY-1 cells were pre-cultured with Z-VAD-FMK (10 mM) for 60 min, and then exposed to BPA (250  $\mu\text{M}$ ) for 24 h. Apoptosis levels were analyzed by TUNEL assay. All bar graphs represent mean  $\pm$  SEM ( $n = 3$  independent experiments). Asterisks indicate significant differences (Student's  $t$ -test,  $P < 0.05$ ).

phosphorylation levels of ERK, p38, and JNK in both normal prostate cell lines, the phosphorylation of AKT was not affected (Fig. 4A-C). Furthermore, the increased phosphorylation levels of ERK, p38, and JNK were reduced in the presence of each inhibitor (U0126, SB203580, and SP600125) (Fig. S4A and F). These findings suggest that the antiproliferative activity of BPA might be associated with the phosphorylation of ERK, p38, and JNK in normal prostate cells.

### 3.5. BPA inhibits potential of wound healing migration and invasion of normal prostate cells via transcription factor-mediated MMP regulation

To evaluate the effect of BPA on the wound healing process, we conducted the wound healing and Boyden chamber assays. In the wound healing assay, BPA significantly inhibited wound closure in WPMY-1 and RWPE-1 cells (Fig. 5A and C). Moreover, the Boyden chamber assay confirmed that BPA impeded the invasive potential compared with untreated cells (Fig. 5B and D). MMP-2 and -9 have been associated with the wound healing process (Aparecida Da Silva et al., 2013; Corbel et al., 2000). Our findings indicate that BPA inhibited the secretion and activity of both MMPs as compared with untreated cells (Fig. 6A-D, Fig. S5A-D). The activation of transcription factors, such as Sp-1, AP-1, and NF- $\kappa$ B, are involved in the regulation of MMPs (Lee et al., 2013; Park et al., 2015). To examine whether BPA affected the binding activity of these transcription factors, we performed EMSA and showed the deactivation of AP-1 and NF- $\kappa$ B activity by BPA, whereas Sp-1 activity remained unchanged in both cell lines (Fig. 6E-F, Fig. S5E-F). Taken together, these results demonstrate that BPA-mediated suppression of the wound healing process may be involved in the inhibition of MMP-2 and -9 expression via transcriptional deactivation of transcription factors AP-1 and NF- $\kappa$ B.

## 4. Discussion

The present study investigated the regulatory mechanism of BPA cytotoxicity in human normal prostate cells WPMY-1 and RWPE-1, which have been used in many previous studies of prostate phenotypes (Bilancio et al., 2017; Huang et al., 2018; Kose et al., 2020; Wu et al., 2011). In addition, this is one of the few studies to explore the action mechanisms of BPA toxicity on prostate cells.

It has already been shown that BPA induces cell cycle arrest, leading to antiproliferative activity (Bilancio et al., 2017; Kidani et al., 2017), but the molecular mechanism underlying BPA-induced G2/M arrest was

largely unknown. The results presented here demonstrate that BPA treatment inhibits the proliferation of both WPMY-1 and RWPE-1 cell lines via ATM-mediated G2/M cell cycle arrest. The CDC2–cyclin B complex is a key regulator for the G2/M cell cycle (Stark and Taylor, 2004). To avoid execution of mitosis at inappropriate points in the cell cycle, the activity of CDC2–cyclin B is strictly controlled. Although it is potentially active upon formation, it is negatively regulated by phosphorylation of CDC2 at Thr-14 and Tyr-15 (Stark and Taylor, 2004). At G2/M, CDC25c, the dual-specificity phosphatase of CDC2, activates CDC2–cyclin B by removing these inhibitory phosphorylations (Stark and Taylor, 2004). Notably, CDC25C is negatively regulated by phosphorylation of its Ser-216 residue. The present study shows that BPA treatment induces activation of ATM and phosphorylation of CHK1 and CHK2, resulting in the phosphorylation of CDC25c at Ser-216. In turn, the inhibitory phosphorylations of CDC2 at Thr-14 and Tyr-15 increased, and the expression of cyclin B decreased in both cell lines. Collectively, our data demonstrated that BPA inhibited cell proliferation by inducing G2/M cell cycle arrest via the ATM–CHK1/CHK2–CDC25c–CDC2 signaling pathway.

DNA damage may lead to transcriptional and replication errors and, if unrepaired or improperly repaired, can ultimately lead to cell death or gene mutation (De Almagro and Vucic, 2012; Yan et al., 2014). DNA single-strand breaks are detected by the Rad9–Hus1–Rad1 complex, which promotes activation of ATR (Yan et al., 2014). DNA double-strand breaks are detected by the Mre11–Rad50–NBS1 complex, which activates ATM (Yan et al., 2014). Our data show that BPA promotes the activation of ATM but not ATR. Based on previous studies and our findings, we postulated that BPA induces apoptosis by stimulating DNA double-strand breaks. The two main components of apoptosis are the extrinsic (DR4/DR5/FAS–caspase-8 cascade) and intrinsic (Bcl-2 family–caspase-9 cascade) pathways, in which the signals that initiate cell death occur either outside or inside the cell, respectively (De Almagro and Vucic, 2012; Yan et al., 2014). BPA treatment increased the expression of apoptosis-related receptors (DR4, DR5, and FAS) in the extrinsic pathway, particularly the expression of TRAIL, a ligand of DR4 and DR5. These receptors activated caspase-8, which triggered downstream caspase-3 and -7, committing the cells to apoptosis. In addition, activated caspase-8 initiated the intrinsic pathways, thereby regulating the Bcl-2 family to activate caspase-9, and this activated caspase-3 and -7 cascades. Finally, activation of the initiator (caspase-8 and -9) and executioner (caspase-3 and -7) caspase cascades led to cell apoptosis. The present data revealed that BPA induces both intrinsic and extrinsic

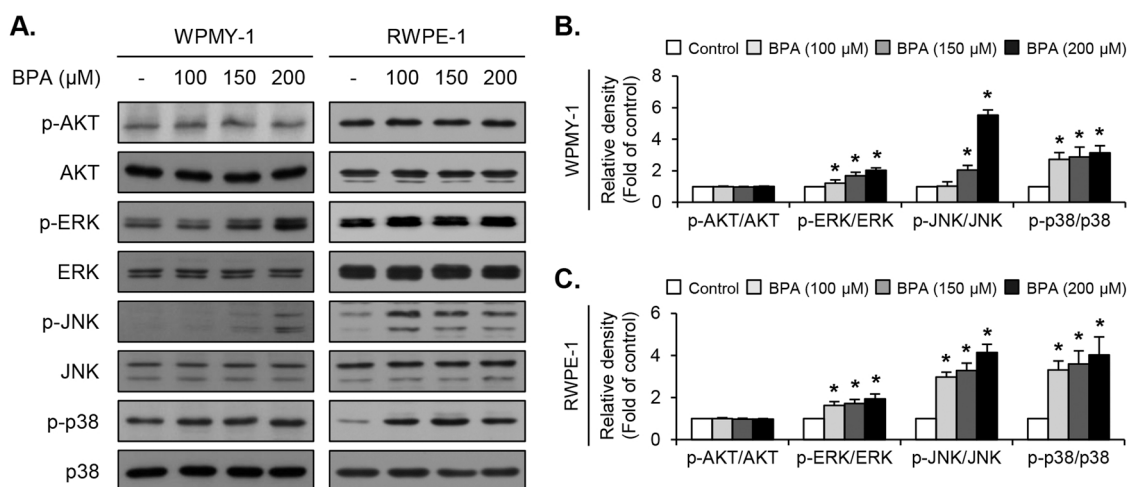


**Fig. 4.** BPA induced differential phosphorylation of signaling pathways in normal prostate cells. (A–C) WPMY-1 and RWPE-1 cells were treated with BPA at 0, 100, 150, and 200  $\mu$ M for 30 min. Phosphorylated and total forms of MAPKs (ERK, JNK, and p38) and AKT were measured by immunoblot analysis. All bar graphs represent the fold change in phosphorylation rates compared to control and present mean  $\pm$  SEM ( $n = 3$  independent experiments). Asterisks indicate significant differences (Student's  $t$ -test,  $P < 0.05$ ).

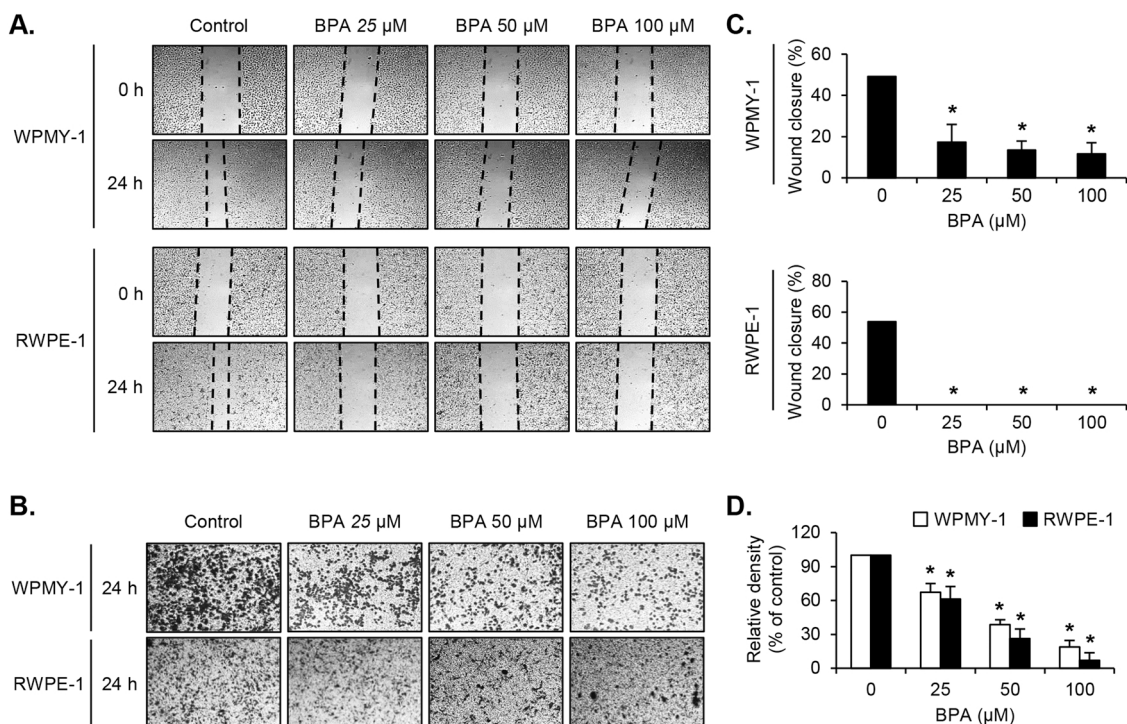


**Fig. 5.** BPA inhibits the wound healing process of normal prostate cells. WPMY-1 and RWPE-1 cells were treated with BPA at 0, 25, 50, and 100  $\mu\text{M}$  for 24 h. The inhibitory effects of BPA on the cell wound healing process were assessed by wound healing assays (A) and invasion assays (B). (C, D) Bar diagrams represent the relative fold changes in wound closure and density of invading cells compared with the control. Graphs represent mean  $\pm$  SEM ( $n = 3$  independent experiments). Asterisks indicate significant differences (Student's *t*-test,  $P < 0.05$ ).

apoptotic pathways, which were associated with induction of the apoptosis-related receptors, regulating the Bcl-2 family, and the activation of initiator and executioner caspase cascades in prostate normal cells.

MAPKs and AKT have been extensively investigated because of their involvement in various cellular events that regulate inflammation, cell differentiation, cell growth, cell cycle arrest, and programmed cell death (Bilancio et al., 2017; Lee et al., 2013; Liu et al., 2013; Park et al., 2015). BPA has already been shown to inhibit the proliferation of human colonic endometrial cells through MAPK and AKT pathways (Wang et al., 2015). It has also been found to inhibit proliferation and induce apoptosis of rat embryonic midbrain cells through the JNK signaling pathways (Liu et al., 2013). Recent studies have shown that MAPK signaling pathways are involved in the bisphenol-induced apoptosis induction in several experimental models (Yuan et al., 2019; Kaur et al., 2021; Huang et al., 2021). The present study demonstrated that BPA treatment induced phosphorylation of ERK, p38, and JNK. Consistent with previous studies, our results suggest that the antiproliferative and apoptosis activity of BPA may be associated with the phosphorylation of MAPKs in prostate cells.

Various complications, such as urinary tract infections, post-operative hemorrhaging, urodynia, and urinary urgency, can occur before complete wound healing after the current gold standard surgical treatments, namely transurethral prostatectomy and thulium laser prostatectomy (Sun et al., 2020; Wang et al., 2017). Therefore, it is especially important to promote prostate wound healing after surgery. Prostates are important target organs for androgen and are induced by androgen and AR pathways to grow and develop (Davis-Dao et al., 2007; Roehrborn, 2008). In a previous study, AR knockout mice showed faster cutaneous wound healing than wild-type mice, indicating that AR signaling has a pivotal role in suppressing cutaneous wound healing (Wang et al., 2017). In line with these results, androgen deprivation accelerates wound healing of the prostatic urethra after a thulium laser prostatectomy (Sun et al., 2020; Wang et al., 2017). It is well known that

BPA acts as an AR antagonist by interfering with AR signaling to arrest AR function (Calafat et al., 2005; Rehan et al., 2015; Welshons et al., 2006). These previous studies point toward the possibility that BPA acts as an AR antagonist, thus accelerating wound healing in the prostate. Normally, degradation of extracellular matrix by MMPs is an important process for the wound-healing capacity (Aparecida Da Silva et al., 2013; Corbel et al., 2000). MMPs, such as MMP-2 and MMP-9, can degrade basement membrane, leading to migration and invasion of several types of cells (Lee et al., 2013; Park et al., 2015). The regulation of MMPs is elaborately involved in the Sp-1, AP-1, and NF- $\kappa$ B transcription factors (Lee et al., 2013; Park et al., 2015). Contrary to what we expected, our data present convincing evidence that BPA interferes with the rapid wound healing process by inducing the inactivation of transcription factor-mediated MMP-2 and -9 in normal prostate cells. Admittedly, the wound healing process is a complicated phenomenon involving many factors. To some extent, the prostate wound healing process is similar to cutaneous wound healing, but it may also be much more complex as wound healing occurs in the male-specific parenchyma of the pelvic cavity. Thus, future studies will be required to examine the exact mechanism involved in the inhibition of prostate wound healing by BPA.

## 5. Conclusions

In conclusion, our study elucidates a circumstantial mechanism by which the toxicity of BPA is implicated in cell proliferation inhibition, apoptosis induction, and wound healing process interference in normal prostate cells. BPA inhibited cell proliferation by inducing G2/M cell cycle arrest via the ATM-CHK1/CHK2-CDC25c-CDC2 signaling pathway. In addition, BPA induced caspase-dependent apoptosis through the initiator (caspase-8 and -9) and executioner (caspase-3 and -7) caspase cascades. Additionally, BPA interfered with the wound healing process through MMP-2 and -9 inactivation by reducing the binding activity of transcription factors AP-1 and NF- $\kappa$ B. Furthermore,

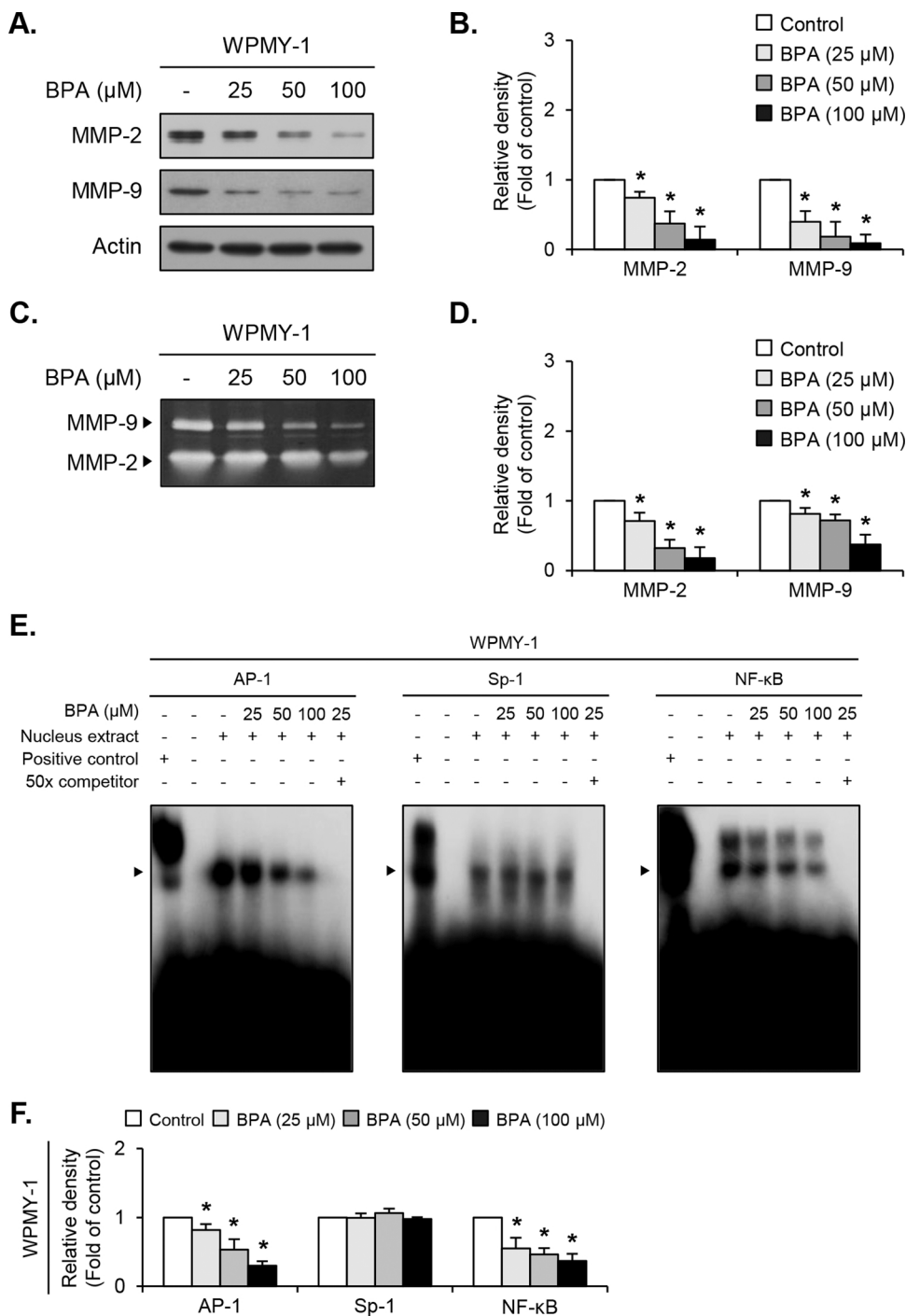


**Fig. 6.** BPA reduces the expression of MMP-2 and -9 by inhibiting AP-1 and NF-κB binding activity. WPMY-1 cells were treated with BPA at 0, 25, 50, and 100 μM for 24 h. (A, B) Expression of MMP-2 and -9 were measured by immunoblot. Bar graphs show relative fold changes in the protein levels at different concentrations of BPA compared with the control. (C, D) Zymographic assay was performed to determine activity of MMP-2 and -9. Graphs show relative proteolytic activity as fold changes in comparison with the control. (E, F) Binding activity of AP-1, Sp-1, and NF-κB was measured by EMSA. Unlabeled AP-1, Sp-1, and NF-κB oligonucleotides were used as 50X competitors. Graphs represent mean ± SEM (n = 3 independent experiments). Asterisks indicate significant differences (Student's t-test, P < 0.05).

the phosphorylation of MAPKs (ERK, p38, and JNK) may be involved in the BPA-induced adverse effects in prostate cells. These findings provide new evidence for further understanding the molecular mechanisms of BPA-induced toxicity in the human prostate.

**CRediT authorship contribution statement**

**Jun-Hui Song:** Conceptualization, Methodology, Formal analysis, Validation, Writing – original draft, Writing – review & editing. **Byungdo Hwang:** Formal analysis, Investigation, Validation. **Su-Bin Kim:** Formal analysis, Investigation, Validation. **Yung Hyun Choi:** Supervision, Validation. **Wun-Jae Kim:** Supervision, Validation. **Sung-Kwon Moon:** Conceptualization, Project administration, Supervision,

Writing – original draft, Writing – review & editing.

**Declaration of Competing Interest**

The authors declare that they have no known competing financial interests or personal relationships that could have appeared to influence the work reported in this paper.

**Data Availability**

Data will be made available on request.

## Acknowledgments

This research was supported by the Basic Science Research Program through the National Research Foundation of Korea (NRF) funded by the Ministry of Education (2018R1A6A1A03025159). This research was also supported by the Chung-Ang University Graduate Research Scholarship in 2021.

## Appendix A. Supporting information

Supplementary data associated with this article can be found in the online version at doi:10.1016/j.ecoenv.2022.114358.

## References

- Aparecida Da Silva, A., Leal-Junior, E.C.P., Alves, A.C.A., Rambo, C.S., Dos Santos, S.A., Vieira, R.P., De Carvalho, P.T.C., 2013. Wound-healing effects of low-level laser therapy in diabetic rats involve the modulation of MMP-2 and MMP-9 and the redistribution of collagen types I and III. *J. Cosmet. Laser Ther.* 15, 210–216.
- Barbalat, Y., Velez, M.C., Sayegh, C.I., Chung, D.E., 2016. Evidence of the efficacy and safety of the thulium laser in the treatment of men with benign prostatic obstruction. *Ther. Adv. Urol.* 8, 181–191.
- Bilancio, A., Bontempo, P., Di Donato, M., Conte, M., Giovannelli, P., Altucci, L., Migliaccio, A., Castoria, G., 2017. Bisphenol A induces cell cycle arrest in primary and prostate cancer cells through EGFR/ERK/p53 signaling pathway activation. *Oncotarget* 8, 115620–115631.
- Brede, C., Fjeldal, P., Skjevraak, I., Herikstad, H., 2003. Increased migration levels of bisphenol A from polycarbonate baby bottles after dishwashing, boiling and brushing. *Food Addit. Contam.* 20, 684–689.
- Calafat, A.M., Kuklennyk, Z., Reidy, J.A., Caudill, S.P., Ekong, J., Needham, L.L., 2005. Urinary concentrations of bisphenol A and 4-nonylphenol in a human reference population. *Environ. Health Perspect.* 113, 391–395.
- Corbel, M., Boichot, E., Lagente, V., 2000. Role of gelatinases MMP-2 and MMP-9 in tissue remodeling following acute lung injury. *Braz. J. Med. Biol. Res.* 33, 749–754.
- Davis-Dao, C.A., Tuazon, E.D., Sokol, R.Z., Cortessis, V.K., 2007. Male infertility and variation in CAG repeat length in the androgen receptor gene: a meta-analysis. *J. Clin. Endocrinol. Metab.* 92, 4319–4326.
- De Almagro, M.C., Vucic, D., 2012. The inhibitor of apoptosis (IAP) proteins are critical regulators of signaling pathways and targets for anti-cancer therapy. *Exp. Oncol. Erickson, B.E., 2008. Bisphenola under scrutiny. Chem. Eng. N.* 86, 36–39.
- Fiege, H., Voges, H., Hamamoto, T., Umamura, S., Iwata, T., Miki, H., Fujita, Y., Buysch, H., Garbe, D., Paulus, W., 2000. Phenol derivatives. *Ullmann's Encyclopedia of Industrial Chemistry*.
- Huang, D., Zheng, C., Pan, Q., Wu, S., Su, X., Li, L., Wu, J., Sun, Z., 2018. Oral exposure of low-dose bisphenol A promotes proliferation of dorsolateral prostate and induces epithelial-mesenchymal transition in aged rats. *Sci. Rep.* 8, 490.
- Huang, M., Li, X., Jia, S., Liu, S., Fu, L., Jiang, X., Yang, M., 2021. Bisphenol AF induces apoptosis via estrogen receptor beta (ERβ) and ROS-ASK1-JNK MAPK pathway in human granulosa cell line KGN. *Environ. Pollut.* 270, 116051.
- Kaur, S., Saluja, M., Aniq, A., Sadwal, S., 2021. Selenium attenuates bisphenol A incurred damage and apoptosis in mice testes by regulating mitogen-activated protein kinase signalling. *Andrologia* 53 (3), e13975.
- Kidani, T., Yasuda, R., Miyawaki, J., Oshima, Y., Miura, H., Masuno, H., 2017. Bisphenol A inhibits cell proliferation and reduces the motile potential of murine LM8 osteosarcoma cells. *Anticancer Res* 37, 1711–1722.
- Kose, O., Rachidi, W., Beal, D., Erkekoglu, P., Fayyad-Kazan, H., Kocer Gumusel, B., 2020. The effects of different bisphenol derivatives on oxidative stress, DNA damage and DNA repair in RWPE-1 cells: a comparative study. *J. Appl. Toxicol.* 40, 643–654.
- Lee, S., Cho, S., Lee, E., Kim, S., Lee, S., Lim, J., Choi, Y.H., Kim, W., Moon, S., 2013. Interleukin-20 Promotes Migration of Bladder Cancer Cells through Extracellular Signal-regulated Kinase (ERK)-mediated MMP-9 Protein Expression Leading to Nuclear Factor (NF-κB) Activation by Inducing the Up-regulation of p21WAF1 Protein Expression\*[S]. *J. Biol. Chem.* 288, 5539–5552.
- Liu, R., Xing, L., Kong, D., Jiang, J., Shang, L., Hao, W., 2013. Bisphenol A inhibits proliferation and induces apoptosis in micromass cultures of rat embryonic midbrain cells through the JNK, CREB and p53 signaling pathways. *Food Chem. Toxicol.* 52, 76–82.
- Park, S.L., Cho, T., Won, S.Y., Song, J., Noh, D., Kim, W., Moon, S., 2015. MicroRNA-20b inhibits the proliferation, migration and invasion of bladder cancer EJ cells via the targeting of cell cycle regulation and Sp-1-mediated MMP-2 expression. *Oncol. Rep.* 34, 1605–1612.
- Rehan, M., Ahmad, E., Sheikh, I.A., Abuzenadah, A.M., Damanhoury, G.A., Bajouh, O.S., AlBasri, S.F., Assiri, M.M., Beg, M.A., 2015. Androgen and progesterone receptors are targets for Bisphenol A (BPA), 4-Methyl-2,4-bis-(P-Hydroxyphenyl)Pent-1-Ene-A potent metabolite of BPA, and 4-Tert-Octylphenol: a computational insight. *PLoS One* 10, e0138438.
- Roehrborn, C.G., 2008. Pathology of benign prostatic hyperplasia. *Int. J. Impot. Res.* 20 (Suppl 3), 11.
- Siegel, R.L., Miller, K.D., Jemal, A., 2020. Cancer statistics. 2020. *CA: a Cancer J. Clin.* 70, 7–30.
- Stark, G.R., Taylor, W.R., 2004. Analyzing the G2/M checkpoint. *Methods Mol. Biol.* 280, 51–82.
- Sun, M., Deng, Z., Shi, F., Zhou, Z., Jiang, C., Xu, Z., Cui, X., Li, W., Jing, Y., Han, B., 2020. Rebamipide-loaded chitosan nanoparticles accelerate prostatic wound healing by inhibiting M1 macrophage-mediated inflammation via the NF-κB signaling pathway. *Biomater. Sci.* 8, 912–925.
- Takahashi, O., Oishi, S., 2003. Testicular toxicity of dietarily or parenterally administered bisphenol A in rats and mice. *Food Chem. Toxicol.* 41, 1035–1044.
- Teng, C., Goodwin, B., Shockley, K., Xia, M., Huang, R., Norris, J., Merrick, B.A., Jetten, A.M., Austin, C.P., Tice, R.R., 2013. Bisphenol A affects androgen receptor function via multiple mechanisms. *Chem. Biol. Inter.* 203, 556–564.
- Wang, K., Kao, A., Chang, C., Lin, T., Kuo, T., 2015. Bisphenol A-induced epithelial to mesenchymal transition is mediated by cyclooxygenase-2 up-regulation in human endometrial carcinoma cells. *Reprod. Toxicol.* 58, 229–233.
- Wang, X., Zhuo, J., Luo, G., Zhu, Y., Yu, D., Zhao, R., Jiang, C., Shi, Y., Li, H., Chen, L., 2017. Androgen deprivation accelerates the prostatic urethra wound healing after thulium laser resection of the prostate by promoting re-epithelialization and regulating the macrophage polarization. *Prostate* 77, 708–717.
- Welshons, W.V., Nagel, S.C., vom Saal, F.S., 2006. Large effects from small exposures. III. Endocrine mechanisms mediating effects of bisphenol A at levels of human exposure. *Endocrinology* 147, 56.
- Wen, X., Zhu, M., Li, Z., Li, T., Xu, X., 2022. Dual effects of bisphenol A on wound healing, involvement of estrogen receptor β. *Ecotoxicol. Environ. Saf.* 231, 113207.
- Wilson, N.K., Chuang, J.C., Morgan, M.K., Lordo, R.A., Sheldon, L.S., 2007. An observational study of the potential exposures of preschool children to pentachlorophenol, bisphenol-A, and nonylphenol at home and daycare. *Environ. Res.* 103, 9–20.
- Wu, J., Jiang, X., Liu, G., Liu, X., He, G., Sun, Z., 2011. Oral exposure to low-dose bisphenol A aggravates testosterone-induced benign hyperplasia prostate in rats. *Toxicol. Ind. Health* 27, 810–819.
- Yan, S., Sorrell, M., Berman, Z., 2014. Functional interplay between ATM/ATR-mediated DNA damage response and DNA repair pathways in oxidative stress. *Cell. Mol. Life Sci.* 71, 3951–3967.
- Yuan, L., Qian, L., Qian, Y., Qian, Y., Liu, J., Yang, K., Huang, Y., Wang, C., Li, Y., Mu, X., 2019. Bisphenol F-induced neurotoxicity toward zebrafish embryos. *Environ. Sci. Technol.* 53, 14638–14648.
- Zalko, D., Jacques, C., Duplan, H., Bruel, S., Perdu, E., 2011. Viable skin efficiently absorbs and metabolizes bisphenol A. *Chemosphere* 82, 424–430.